Fatigue Study Of *E*-Glass Fiber Reinforced Polyester Composite Under Fully Reversed Loading And Spectrum Loading

Dr. Muhannad Z. Khelifa* **Hayder Moasa Al-Shukri****

Received on: 3/12/2007
Accepted on:6/4/2008

Abstract

Study of the fatigue behaviors experimentally and theoretically of a composite material manufactured for this paper by stacking four layers of E-glass fiber in different angle orientations ($0^o, \pm 45^o$, $0^o/90^o$) immersed in polyester resin with total thickness 4 mm. They were tested under two types of dynamic loads in fully reversible tension-compression load at (R=-1) and spectrum load as fatigue testing, to estimate life curves and microscopic an examination was carried out for stress affected and fracture areas. Finite Element Analysis (FEA) using ANSYS Workbench™ was used to evaluate the composite behaviour under fatigue conditions. The results of the fatigue test show that the uniaxial [04] composite has the highest strength and the fatigue degradation is also the highest. The high magnification optical microscopy method shows that the failure of laminas at $\pm 45^o$and $0^o/ 90^o$ is due to matrix failure in the direction of the fiber, whereas for the unidirectional lamina at 0^o, the failure is due to fiber breakages.

Keywords: E-Glass fiber, Composite material fatigue, Spectrum Loading, Fully reversed Loading (tension-compression).

دراسة الكلال لمادة الليف الزجاجي المدعوم بالبولستر المصنعة عند التحميل (الشد- انضغاط) المعكوس والتحميل الطيفي

الخلاصة

دراسة سلوك الكلال عمليا و نظريا لمادة مركبة مصنعة لهذا البحث مكونة من أربعة طبقات من الليف الزجاجي و باتجاهات مختلفة الزوايا($0^o/90^o \pm$), (45^o, 0^o) مغمور بمادة البوليستر وذات سمك كلي 4 ملم وتم اختبارها تحت نوعين من الأحمال الديناميكية,حمل متعاكس (شد – انضغاط)عند (R=-1) وحمل طيفي كاختبار الكلال وذلك للحصول على مخططات العمر وكذلك أجراء الفحص ألمجهري للمناطق المعرضة للإجهاد والكسر.التحليل النظري بطريقة العناصر المحددة تم باستخدام برنامج الحاسبة الجاهز ANSYS Workbench® وذلك لتقيم سلوك المادة المركبة في حالات اختبار الكلال. أظهرت نتائج فحص الكلال إن نموذج المادة المركبة المصنعة ذات الاتجاه الواحد [04] لها اكبر قوة متانة وكذلك أعلى انحدار بالطاقة . أن طريقة الفحص ألمجهري البصري بينت فشل الكلال في منطقة التخصر في العينات المفحوصة (45^o, $0^o/90^o \pm$) في المادة الرابطة ثم في الألياف بينما العينات ذات الاتجاه الواحد (0^o) فان الكلال يظهر عند الألياف.

Notation

a, b	Curve fitting parameters	–
c , d	Regression constants	–
$E_{i,i}$	Young's modulus of elasticity in the directions *i, j=1,2,3* local coordinate directions	N/m^2

https://doi.org/10.30684/ etj.26.10.6
University of Technology-Iraq, Baghdad, Iraq/2412-0758

$G_{i,j}$	Shear modulus in local and global coordinates	N/m^2
$M_{f,m}$	Weight fraction of fiber, and matrix, respectively	_
N	Number of laminate's layer	_
R	Stress ratio	_
V_f, V_m	Volume fraction of fiber , and matrix respectively	_
W_f	Wight fraction	_
w_f, w_m	Mass of fiber, and matrix respectively	Kg
X_t, (X_c)	Longitudinal tensile (compressive) strength	N
$v_{c,f,m}$	Volume of composite, fiber, and matrix, respectively	m^3
$\rho_{c,f,m}$	Density of composite, fiber, and matrix, respectively	gm/cm^3
$\sigma_{f,m}$	Stress on fiber , and matrix respectively	N/m^2
$v_{i,j}$	Poisson's ratio in the local and global coordinate directions	_
$\gamma_{i,j}$	Shear strain in the local and global coordinate directions	_
$\iota_{i,j}$	Shear stress in the local and global coordinate directions	N/m^2
σ_{ult}	UTS, ultimate tensile stress N/m^2	
σ_{max}	Maximum stress	N/m^2
σ_{min}	Minimum stress	N/m^2

Introduction

Knowledge of the damage mechanisms and their progression is to understand the fatigue behaviour of composite materials, these damage mechanisms are abundant, they occur at many unpredictable locations throughout the laminate. There are five major damage mechanisms: matrix cracking, fiber breaking, crack coupling, delamination beginning, and delamination growth [1]. Van and Degrieck (2001) [2] investigated fatigue test on the specimens which have *8*-layer plain-woven glass epoxy composite [0_8], they reported the bending fatigue performance of the composite from experimental tests on straight specimens. These specimens degrade gradually and their stiffness is reduced significantly after $4*10^5$ cycles. Although the $[\pm 45]_8$ specimen is not as strong and stiff to start with, after $3*10^5$ cycles, their remaining stiffness is greater than that of the [0_8] specimens. Furthermore, a considerable deformation remained after removing the grips from the $[\pm 45]_8$ specimens while this was not the case in the [0_8] specimens. Wahl et al (2002) [3], considered lamnate of E-glass reinforced thermoset matrix ($V_f = 0.36$) to demonstrate the progression of fatigue damage at constant amplitude and at block spectra to include high and low cycle spectrum. A database was generated from measurements made on over *1100* lab specimens in order to establish the required design conditions that provide a desired lifetime of wind turbine that exceeds *30* years (10^9 *cycles*). Wahl, and Samborsky (2003) [4] extended their work to include simple spectra which cover a full range of loads including compression and reversed tension-compression as well as other spectra that covers a full range of R-values. The effect of modeling assumptions on the accuracy of spectrum fatigue

lifetime predictions is documented. Freire (2005) [5] investigated the damage mechanism and failure prevention in E-glass polyester resin composites, his work was limited to bidirectional and stacked bidirectional-woven fabric textile. Tensile (*R=0.1*), compression (*R=10*) and alternate axial (*R=-1*) fatigue test were performed at different maximum stress loads.

In this work the topic has been divided into two parts, experimental and theoretical investigations into the fatigue behaviour of polymer-glass composites under two types of dynamic loads, in fully reversible tension-compression load and spectrum load for understanding the effect of fibers orientation in the laminate.

Theoretical Analysis Volume and Weight Fraction of Aligned Continuous Fiber

To define the fiber volume fraction V_f and the matrix volume fraction V_m consider a composite consisting of fiber and matrix, [6].

$$V_m = \frac{\upsilon_m}{\upsilon_c} = \frac{A_m}{A_c} \quad .....(1.a) \text{ and}$$

$$V_f + V_m = 1 \quad .....(1.b)$$

The mass fraction (weight fraction) of the fibers (M_f) and the matrix (M_m) are defined as:

$$M_f = \frac{w_f}{w_c} \quad ...(2.a) ,$$

$$M_m = \frac{w_m}{w_c} \quad ...(2.b) \text{ and}$$

$$M_f + M_m = 1 \quad ...(2.c)$$

of a single material in terms of the fiber From the definition of the density and matrix volume fractions:

$$M_m = \frac{\rho_m}{\rho_c} V_m \quad ...(3.a) \text{ and}$$

$$M_f = \frac{\rho_f}{\rho_c} V_f \quad ...(3.b)$$

In terms of individual constituent properties, the mass fractions and volume fractions are related by:

$$M_f = \frac{V_f}{V_f + \frac{\rho_m}{\rho_f}(1 - V_f)} \quad ...(4.a),$$

$$V_f = \frac{M_f}{M_f + (1 - M_f)\frac{\rho_f}{\rho_m}} \quad ...(4.b)$$

The density of the composite ρ_c in terms of the constituents' weight fractions and densities can be defined as:

$$\rho_c = \frac{1}{\frac{M_f}{\rho_f} + \frac{M_m}{\rho_m}} \quad ..... (5)$$

It is evident that volume and mass fractions are not equal and that the mismatch between the mass and volume fractions increases as the ratio between the density of fiber and matrix differs from one.

Experimental Procedure

(i). Selection Materials

E-glass fibres having density of 2.5 g/cm^3 and modulus of 72 GPa were used as a reinforcing material in polyester matrix. The polyester,

Syropole 8340 is an unsaturated resin with catalyst addition; having a density of 1.22 g /cm^3 and elasticity modulus 2.82 GPa was used as the matrix material, [7].

(ii).Specimen Preparation

Composite panels were prepared according to ASTM standard D5687 [8] and through a hand lay-up process. The panel thickness and lamina orientations were controlled by performing the lay-up process in a specially made mold frame. The frame was manufactured from steel plate in the workshop with two thicknesses *6 mm* for the base and *12 mm* for the heavy weight cover, net moulding area was *30*30 cm*^{2}. The layers thickness was controlled to *1 mm* by using a steel ruler fixed to the frame, *12* vertical fastener bolts were welded in the base for tighten in the rulers to keep the fibres strung as shown in Figure (1). The cover was applied to prevent any buckling occurring during the curing process. The curing process was completed in 24 hrs at room temperature, followed by oven cure at 70C^o for three hours. The specimens were cut out of the 30x30 cm panels according to ASTM D3479-76 standards [9]. The specimens were dog-bone shaped with the dimensions shown in Figure (2). Four layer composite specimens were prepared at a layer thickness of 1mm. [+45]s, [0/90]s, and [04] composite laminates were prepared and used in the paper. The difference is the weight fraction M_f of the fibre in the composite However, this facility was not available and an alternative method was used by weighing the fibres before lay-up and then weighting the composite panel after curing and calculation using strength ratio mechanics (SRoM) formula given in equation (4).

a-Fiber weight before lay-up was (*110.76*) *gm.*

b-Composite panel weight after curing was (*318.5*) *gm*

c-Then W_f*=0.3478*, which gives a volume fraction value of about (*0.202*).

The volume fraction of the fibre in the composite was 0.22. The engineering constants of the laminates were extracted from tensile measurements,[7] and are given in Table (1).

(iii).Test Equipment and Fatigue Test Procedure

An *Avery Fatigue Testing Machine Type-7305* as shown in figure (3) was used to test the composite laminates. The machine is designed to apply constant amplitude reverse loads with R= -1, where R is given by the ratio of the minimum stress to maximum stress applied to the samples under fatigue tests.

$$R = \frac{\sigma_{\min}}{\sigma_{\max}} \qquad \ldots\ldots (6)$$

Grips are provided for the bend test where the load is imposed at one end of the specimen by an oscillating spindle driven by means of a connecting rod, crank and double eccentric attachment. The eccentric attachment is adjustable to give the necessary range of bending angle. The applied load is measured at the opposite end of the specimen by means of a *Torsion Dynamometer*. The angle of twist is registered on a dial gauge.

Calibration curves giving the relationship between the dial gauge reading and the imposed torque are provided. A revolution counter is fitted to the motor to record the number of cycles, the cycling rate was 1420 rpm.

Fatigue Test Analysis and Results

(i). Optical Microscopy Analysis

Optical microscopic examinations of some specimens subjected to fatigue test indicated that the strongly orthotropic or transversely isotropic properties resulted in the formation of damage zones which contained a multiple of macroscopic cracks Figure(4a), fibre/matrix interface debondings and delamination Figure(4b), pull out of fibres from the matrix Figure (4c), and arrangement of fibres distribution Figure (4d). This damage may have started very early in the test and followed by a gradual degradation and reduction of the stiffness, which finally culminates in fibre breakage and catastrophic failure.

(ii).Fatigue Life Test Analysis

The applied stress was initially estimated from the applied bending moment, using the *Classical Lamination Theory* which assumes a simple rectangular cantilever beam. ANSYS Workbench™ finite element analysis (FEA) commercial tools was then used to recalculate the stress due to the complex shape of the specimen, hence a more accurate stress values were obtained. The constant amplitude fatigue data are summarised in S-N diagrams based upon two regression trends, power and logarithmic-linear laws. These formats of regression trends are typical for fatigue data presentation, [10].

The power law regression equation is:

$$\sigma = a\, N^{\,b} \quad \ldots..(7)$$

The linear-logarithmic law regression equation is:

$$\sigma = c + d\ \log(N) \quad \ldots(8)$$

Where: c and d are the regression constants representative of the trend of fatigue. N is the number of cycles at failure.

The S-N curves are given in Figure (5). The regression constants representative of the fatigue trends from the two models are given in Table (2). The constant (a) in the power law and the coefficient (c) in the logarithmic law are related to the static bending strength. The constants (b) and (d) are related to the fatigue degradation and describe the fatigue sensitivity. It can be seen that the [02]s and [0/90]s samples have the highest bending strength but also the highest degradation rates. However, the [+45]s sample has the lowest static strength, but degrades more slowly under cyclic loading conditions. This is in agreement with the results of Van and Degrieck [2] on $[0]_8$ and $[45]_8$ glass epoxy composites under fully reversed bending fatigue loading (R=-1).

(iii).Fatigue-life Diagram

Fatigue-life diagram is often used to interpret the fatigue failures in tensile fatigue of composites [11]. The S-N data of all laminates are plotted on the same graph in Figure (6). The diagram consists of three distinct regions, each associated with a different set of operative damage mechanisms.

These regions are enumerated as Regions I, II, III.

Fatigue life data for the glass polyester composite presented themselves in these regions with discontinuities in the S-N curve. In region I, the stress level generally coincided with the scatter band of the static stress to failure. Region II, approximately above $5x10^4$ cycle, is called the progressive damage region II. Fatigue sensitivity is generally characterised by the slope in a fatigue-life diagram. Such slope implies that there have been progressive damage mechanisms and the progression rate depends on the applied load level. Fatigue limit above 10^6 cycles is expected to be within an infinitely long time. This region is called Region III. The stress level in this region is expected to be so small that damage does not develop at all, and the composite materials behave in a perfectly elastic manner in cyclic loading.

The three regions of the fatigue behaviour could be attributed to the initial damage of the polyester matrix at the high load. These results in the first drop for endurance in the first few hundred cycles. The reinforcing fibre in this region remains undamaged. Some propagation of the damage in the form of delamination occurs without affecting the bulk of the specimens. The stress cycles being accommodated by the fibres and the residual good adherence between the fibres and the polyester matrix. As the progressive endurance increases at lower subcritical stress level (region I) the failure is due to primary debonding occurring in larger volume across the samples.

The fibre damage begins to occur once the number of fatigue cycles reaches sufficient numbers and combined matrix and fibre damages predominate giving rise to the rapid weakening of the composites (region II). The fibre damage is the consequence of the cumulative residual stresses. Finally in region III, the fatigue stress cycles are inadequate to cause sufficient damage to the fibre and resin matrix, hence sustaining the composite for a good endurance limit.

Fatigue Life and Fatigue Damage Sensitivity Simulations

The experimentally determined S-N curves along with the mechanical properties of the composite laminates given in Table (1) were used to simulate the life-fatigue sensitivity of the composite. Finite Elements ANSYS Workbench™ commercial analytical tool was used in the simulations. Two methods were used in order to determine the fatigue life and the fatigue sensitivity for two types of loading conditions. The loads were applied at the free end of the dog-bone shaped specimens, as following:

(i).Constant Amplitude Loading

A fully reversed (R=-1) sinusoidal load of 1 N.m was used for all laminates to simulate the fatigue test conditions. The contour plots of the available life fatigue for the three types of laminates are given in Figures (7). In these plots, the region of the structure which has the lower cycles to failure is the weakest and will fail first. These failure regions occur in the middle section of the specimens, consistent with the experimental observations.

The curves of fatigue life sensitivity to the applied constant amplitude cyclic reversed loading (R= -1) for the three considered composite specimens, are shown in Figures (8). These plots indicate how the minimum fatigue cycles to failure in the structure change as a function of the applied loading in the range of 0.2 to 2.8 N.m. It can be seen that for cycles $>10^5$, the [04] laminate can sustain the highest fatigue bending loads, whereas the [+45]s laminate sustains the lowest loads. These results are consistent with the experimentally determined S-N curves.

(ii).Spectrum Loading

A non-constant amplitude loading was applied, where the loading spectrum is random in nature. The fatigue life data are presented in contour plots and depicted in Figure (10) for the three types of the composite laminates considered in the investigations. The contours show similar stress patterns to those for the constant amplitude cyclic loading shown in Figure (7).

The fatigue sensitivity to spectrum loading was evaluated by applying loading scale factors of 0.2 to 2.8, to the alternating and the mean values of the spectrum load. The fatigue sensitivity curves are shown in Figures (10) for the three considered composite laminates. It can be seen that, under spectral load conditions, for fatigue cycle $>10^6$ the $[0_2]_s$ laminate sustains the highest loads.

Conclusions

The fatigue results concluded that

1- While the unidirectional $[0^o]_s$ and cross-ply $[0/90]_s$ composite laminates had the highest static bending strength, they degraded fastest under fully reversed bending load.

2- The $[\pm 45]_s$ composite laminate had the lowest strength but the degradation was the slowest.

3-Finite element analysis (FEA) of the fatigue life at constant amplitude load and at variable amplitude spectrum load, have showed that the minimum fatigue cycle to failure occurred at the middle region of the structure.

4- The theoretical analysis consistent with the experimental observation of fatigue failure under fully reversed bending load and the simulation results showed that $[0^o]_s$ laminate sustained the highest load for the longest fatigue life times under both constant amplitude and spectrum loads, whereas the $[\pm 45]_s$ laminate sustained the lowest loads.

References

[1]. Barbero, E. J. "Introduction to Composite Materials Design", Materials Science and Engineering Series,. 1st edition, Taylor & Francis, Inc, 1998.

[2]. Van Paepegem, W., and Degrieck, J. "Experimental setup for and numerical modelling of bending fatigue experiment on Woven Glass/Epoxy Composites", Composite Structure, Vol.51 (1), pp.1-8, 2001.

[3]. Wahl, N. W.,John,K.Z. and Hake,M.F., "Spectrum Fatigue Lifetime and Residual Strength for Fiberglass Laminates", Contractor Report SAND2002-0546, Sandia National Laboratories, Albuquerque, NM, 2002.

[4]. Wahl, N. W. and Samborsky, D. D. "Effect of Modeling Assumptions on the Accuracy of Spectrum Fatigue Lifetime Predictions for a Fiberglass Laminate", AIAA,Vol.0023, 2003.

[5]. Freire, R. C., and Aquino E. F. "Fatigue Damage Mechanism and Failure Prevention in Fiberglass Reinforced Plastic", Materials Research, Vol. 8, No. 1, 45-49, 2005.

[6]. Hull, D. and Clyue, T.W. "An Introduction to Composite Materials" 2nd edition Cambridge solid-state science, series, 1996

[7]. Hayder Al-Shukri," Experimental and Theoretical Investigation into Some Mechanical Properties of E-glass Polyester Composite under Static and Dynamic Loads", MSc Thesis, Engineering Electromechanics Department, University of Technology ,2007.

[8]. http://mihd.net/yn9up8, ASTM D5687/D5687M-95, "Standard Guide for Preparation of Flat Composite Panels with Processing Guidelines for Specimen Preparation",. Book of Standards Volume: 15.03.. 2007.

[9].http://mihd.net/yn9up8,AST M D 3479/D 3479M , "Standard Test method for Tension-Tension for Fatigue of Polymer Matrix Composite Materials". Revision 76., 2007.

[10]. Groover, M. P., "Fundamentals of Modern Manufacturing", 2nd Edition. John Wiley & Sons Inc, 2002.

[11]. Rita R., and BOSE N. R., " Behaviour of *E*-glass fibre reinforced vinylester resin composites under fatigue Condition", Bull. Mater. Sci., Vol. 24, No. 2, pp. 137–142 April 2001.

Table (1) Mechanical Properties of Composite Laminates,[7].

laminates	E_1 (GPa)	E_2 (GPa)	E_3 (GPa)	G_{12} (GPa)	G_{13} (GPa)	G_{23} (GPa)	ν_{12}	ν_{13}	ν_{23}
$[0]_s$	18.04	3.74	3.74	1.57	1.57	1.49	0.34	0.34	0.25
$[-45/45]_s$	5.03	5.03	6.75	4.93	1.53	1.53	0.21	0.15	0.15
$[0/90]_s$	11.04	11.04	6.75	1.57	1.53	1.53	0.12	0.32	0.32

Table (2) Regression Parameters of Fatigue Data

Specimens	Power Law		Logarithmic Law	
	a	*b*	*c*	*d*
$[0_2]_s$	$3.4x10^4$	- 0.62	274.18	- 48.88
$[0/90]_s$	$2.2x10^4$	- 0.61	221.51	- 39.73
$[+45/-45]_s$	$2.7x10^2$	- 0.23	79.24	- 11.74

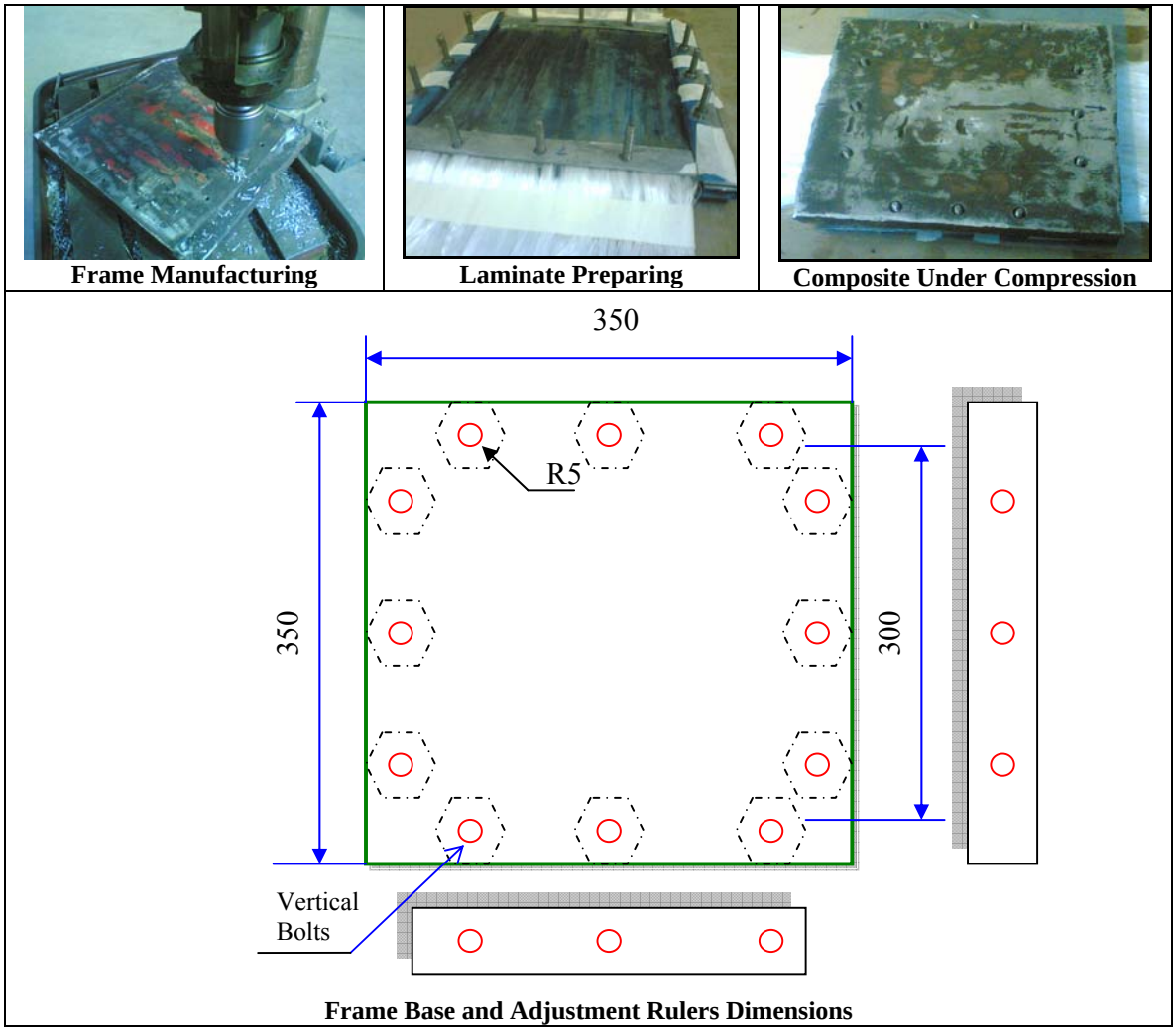

Figure (1) Manufacturing Process and Frame Dimensions

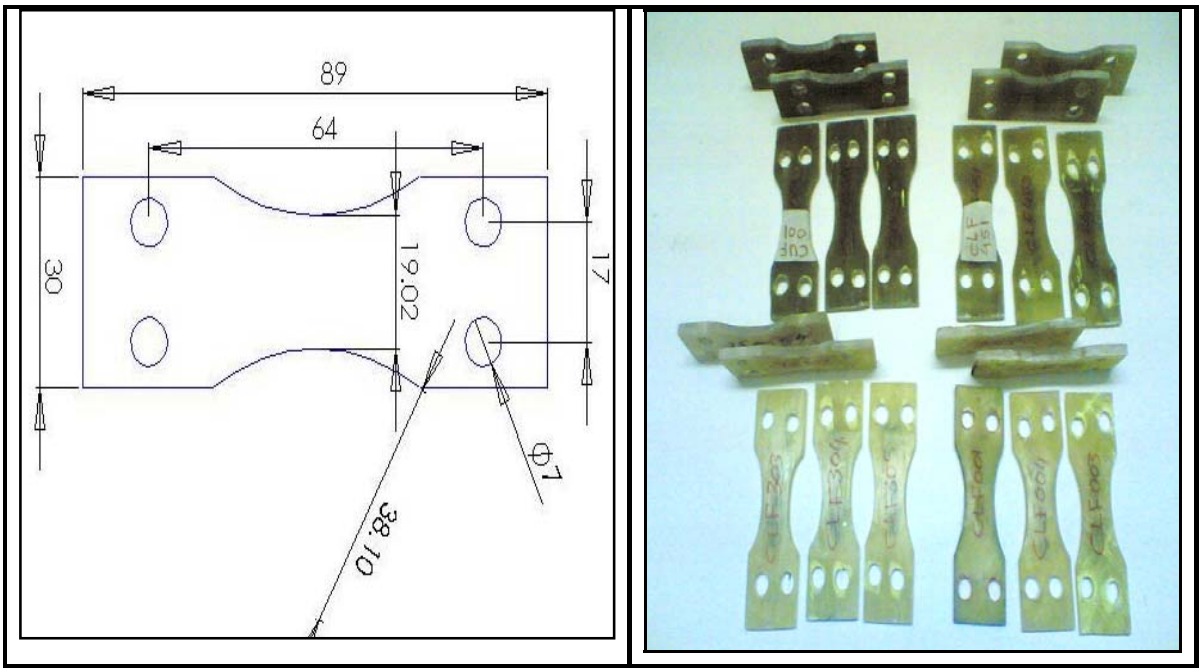

Figure (2) Fatigue Specimens (all dimension in *mm*)

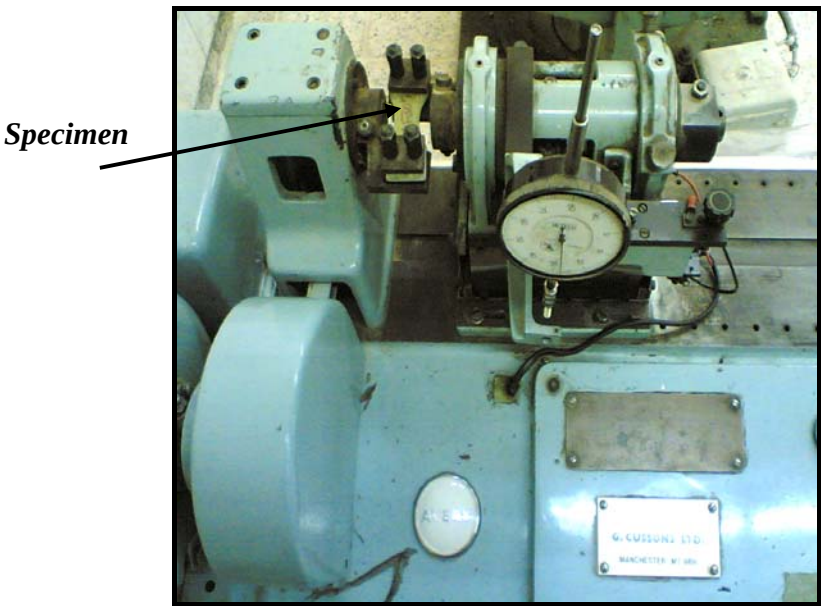

Figure (3) AVERY Fatigue Testing Machine Type ***7305***

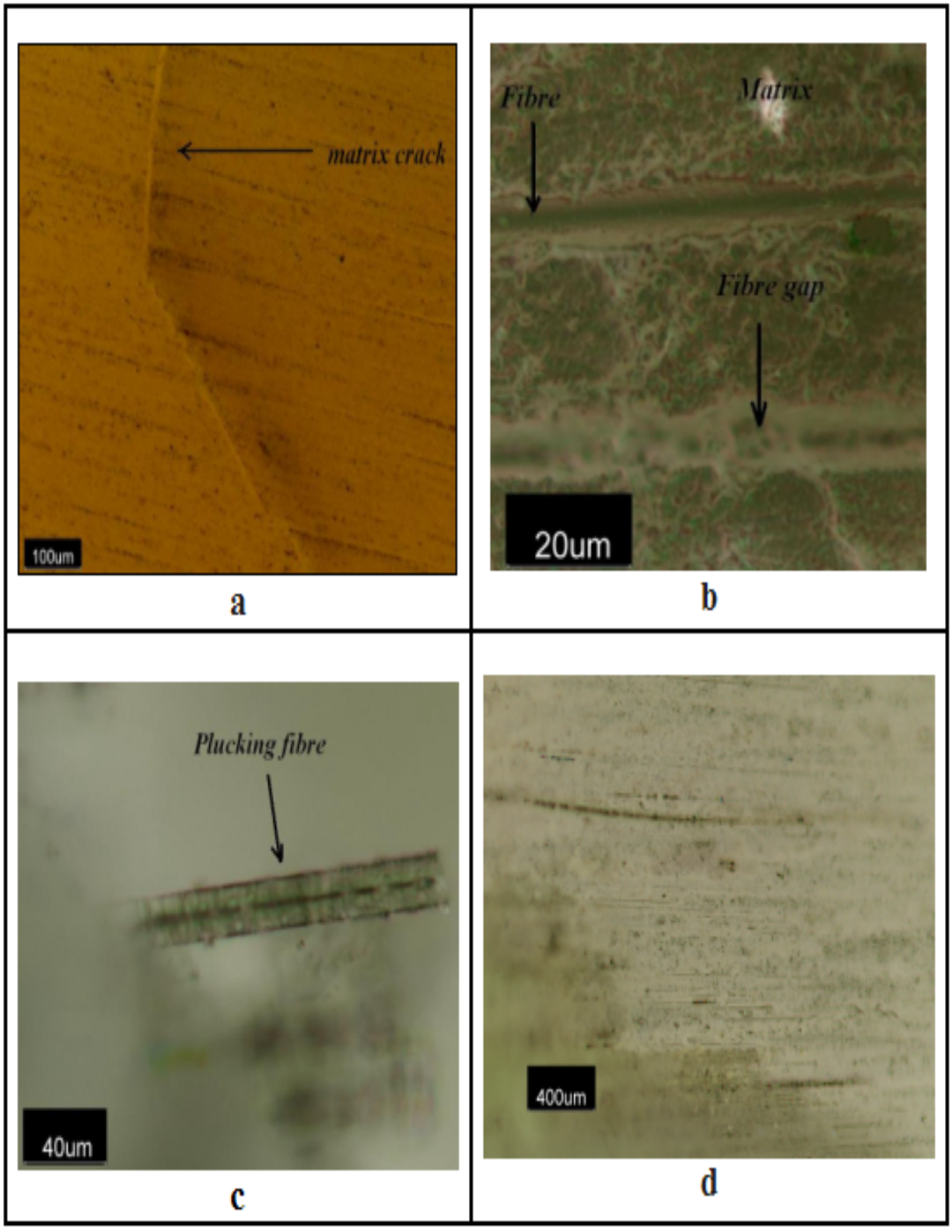

Figure (4) Micrographs of Fatigue Failure Observed in Glass Polyester Composites.
a. Matrix Microcracks. b. Fibre/Matrix Interface Delamination
c. Pull-out of Fibres from Matrix. d. Arrangement and Fibres Distribution.

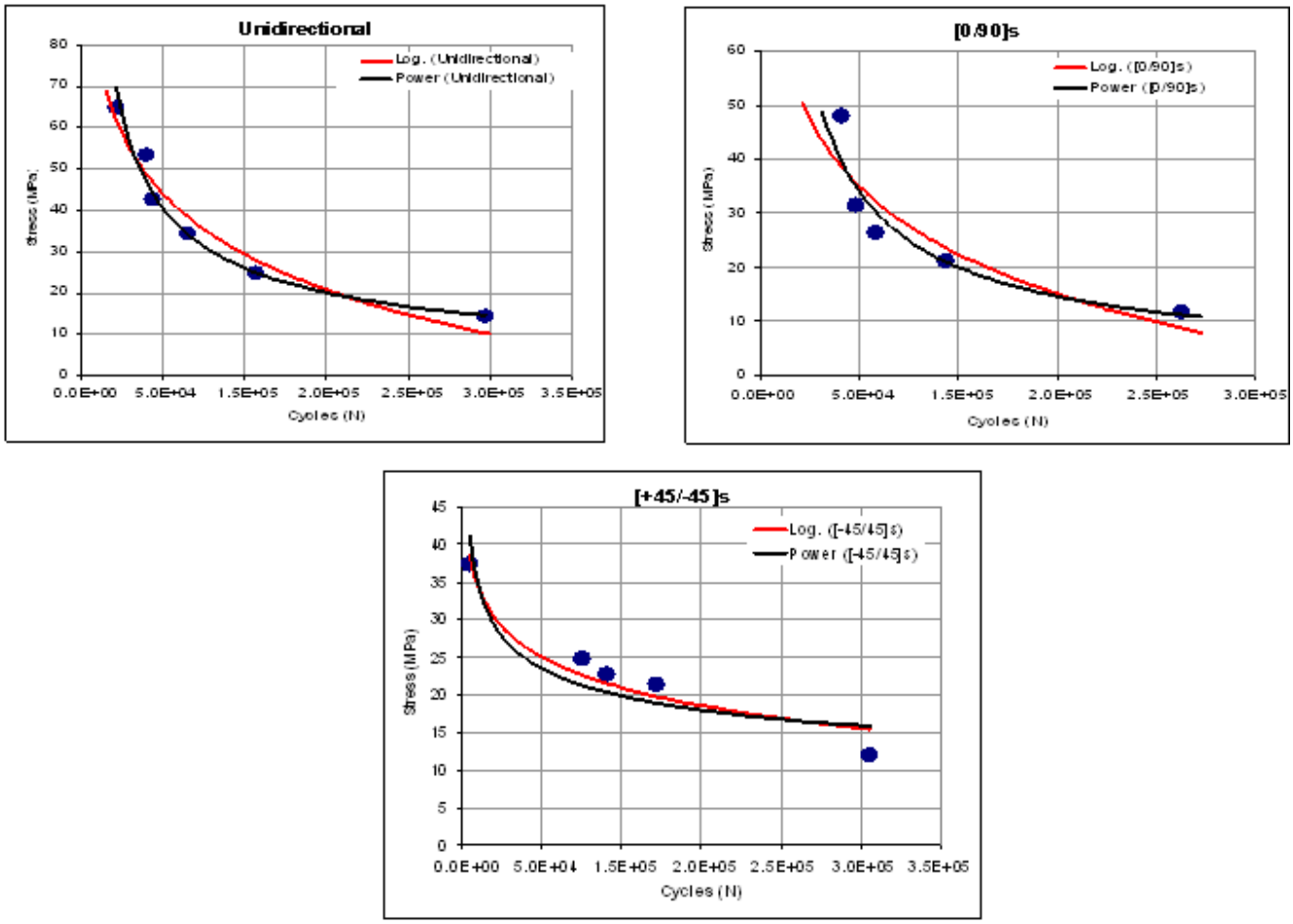

Figure (5) Fatigue Test Results of Glass Polyester Composite Specimens Under Constant Amplitude and Fully Reversed Loading (R=-1)

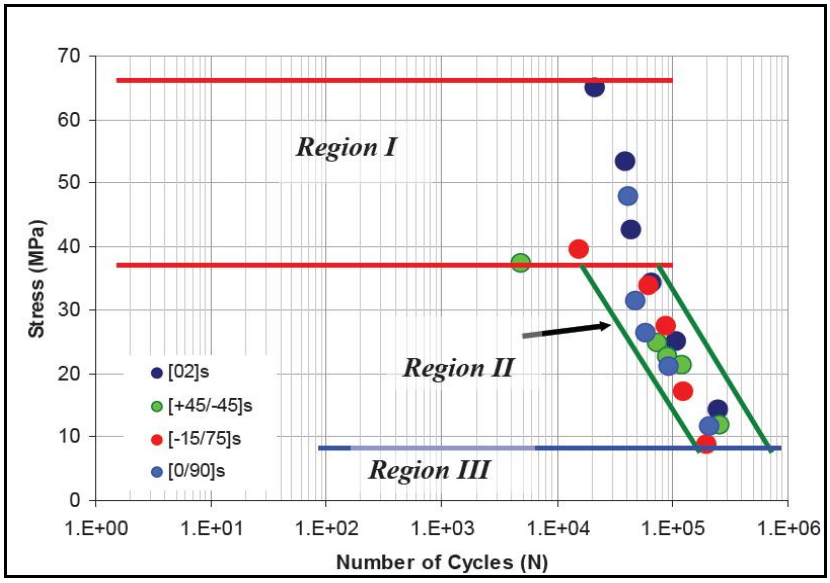

Figure (6) Fatigue-Life Diagram

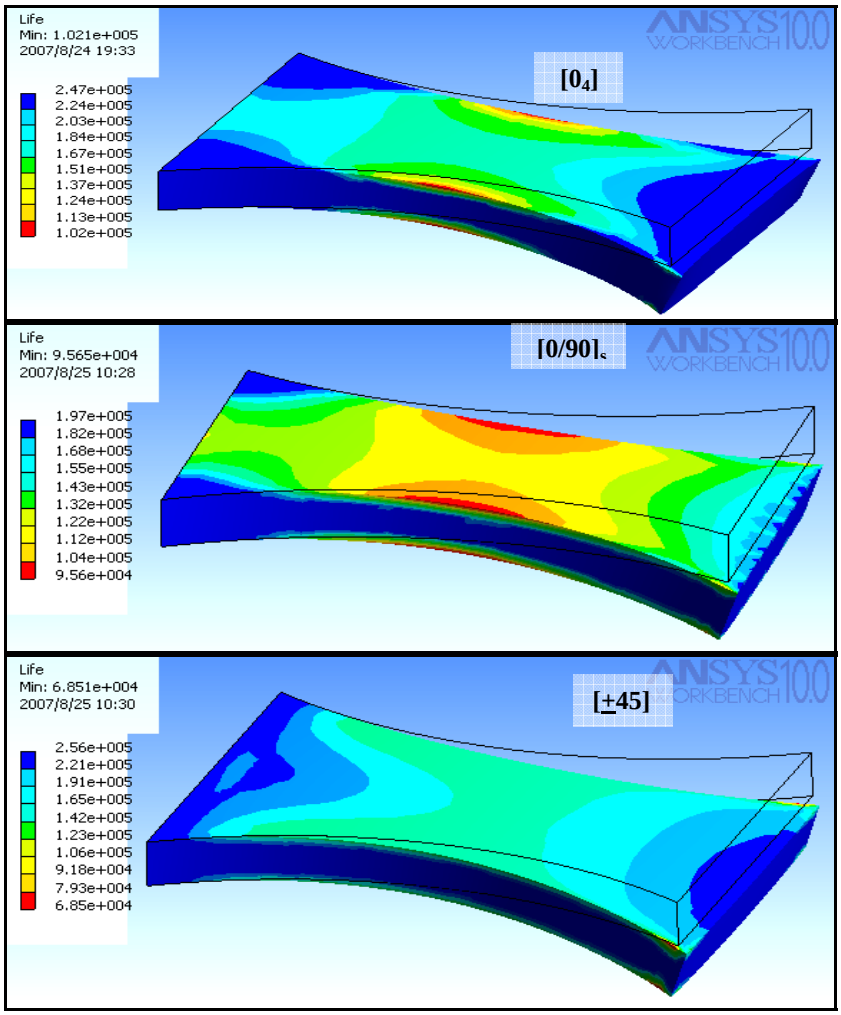

Figure (7) Fatigue Life Contour Plot of
Laminates under Constant Amplitude Loading (R=-1)

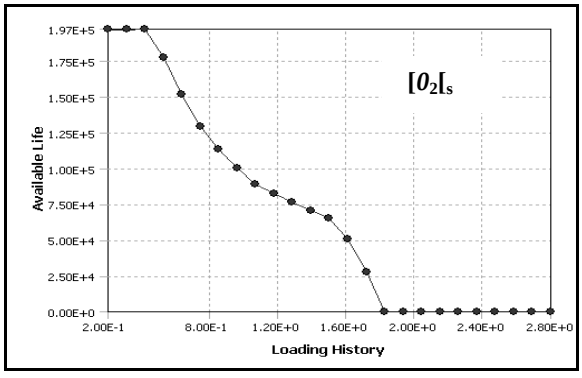

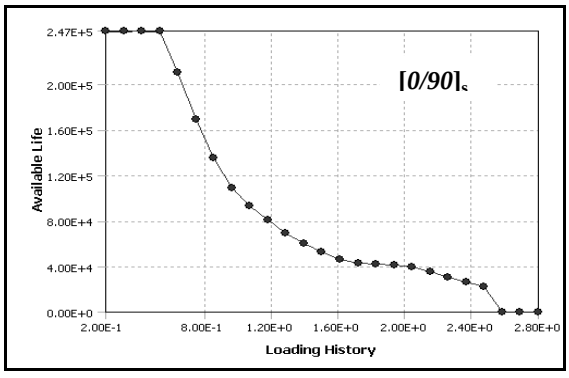

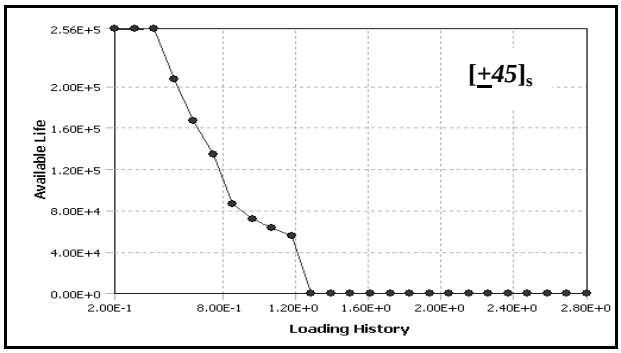

Figure (8) Fatigue Life Sensitivity of Laminates

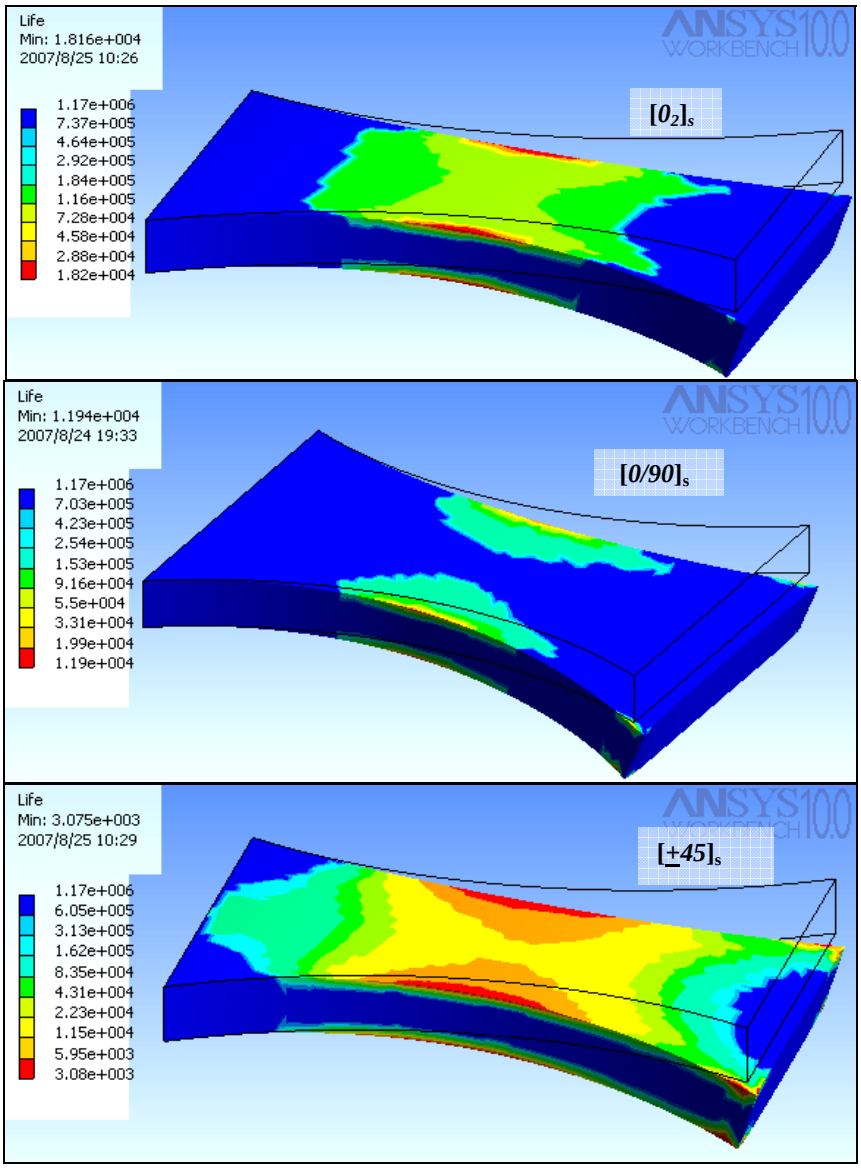

Figure (9) Fatigue Life Contour Plot of Laminates under Spectrum Loading

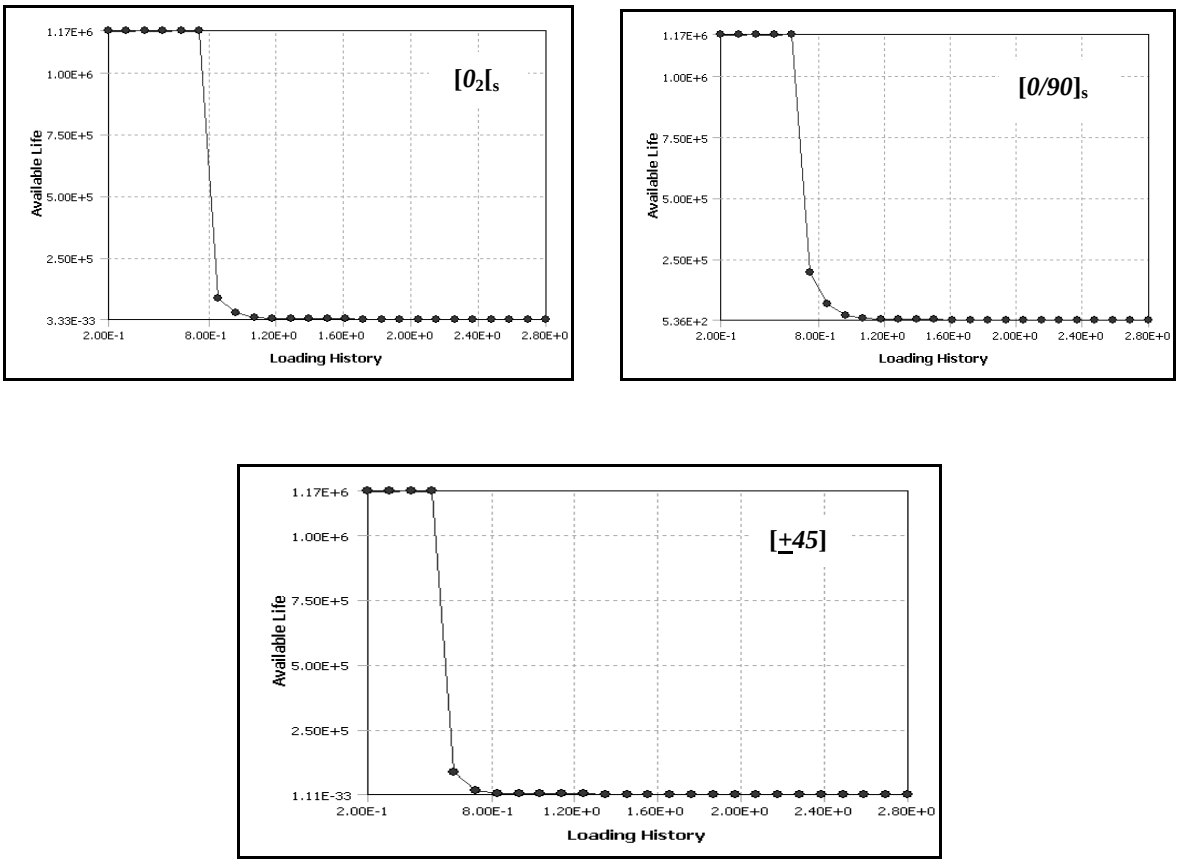

Figure (10) Fatigue Life Sensitivity of Laminates.